

CLNS 97/1497
CLEO 97-16

Study of the Decay $\tau^- \rightarrow 2\pi^-\pi^+3\pi^0\nu_\tau$

CLEO Collaboration

(October 17, 2018)

Abstract

The decay $\tau^- \rightarrow 2\pi^-\pi^+3\pi^0\nu_\tau$ has been studied with the CLEO II detector at the Cornell Electron Storage Ring (CESR). The branching fraction is measured to be $(2.85 \pm 0.56 \pm 0.51) \times 10^{-4}$. The result is in good agreement with the isospin expectation but somewhat below the Conserved-Vector-Current (CVC) prediction. We have searched for resonance substructure in the decay. Within the statistical precision, the decay is saturated by the channels $\tau^- \rightarrow \pi^-2\pi^0\omega\nu_\tau$, $2\pi^-\pi^+\eta\nu_\tau$, and $\pi^-2\pi^0\eta\nu_\tau$. This is the first observation of this ω decay mode and the branching fraction is measured to be $(1.89^{+0.74}_{-0.67} \pm 0.40) \times 10^{-4}$.

S. Anderson,¹ Y. Kubota,¹ S. J. Lee,¹ J. J. O'Neill,¹ S. Patton,¹ R. Poling,¹ T. Riehle,¹
 V. Savinov,¹ A. Smith,¹ M. S. Alam,² S. B. Athar,² Z. Ling,² A. H. Mahmood,²
 H. Severini,² S. Timm,² F. Wappler,² A. Anastassov,³ J. E. Duboscq,³ D. Fujino,^{3,*}
 K. K. Gan,³ T. Hart,³ K. Honscheid,³ H. Kagan,³ R. Kass,³ J. Lee,³ M. B. Spencer,³
 M. Sung,³ A. Undrus,^{3,†} R. Wanke,³ A. Wolf,³ M. M. Zoeller,³ B. Nemati,⁴ S. J. Richichi,⁴
 W. R. Ross,⁴ P. Skubic,⁴ M. Bishai,⁵ J. Fast,⁵ J. W. Hinson,⁵ N. Menon,⁵ D. H. Miller,⁵
 E. I. Shibata,⁵ I. P. J. Shipsey,⁵ M. Yurko,⁵ L. Gibbons,⁶ S. Glenn,⁶ S. D. Johnson,⁶
 Y. Kwon,^{6,‡} S. Roberts,⁶ E. H. Thorndike,⁶ C. P. Jessop,⁷ K. Lingel,⁷ H. Marsiske,⁷
 M. L. Perl,⁷ D. Ugolini,⁷ R. Wang,⁷ X. Zhou,⁷ T. E. Coan,⁸ V. Fadeev,⁸ I. Korolkov,⁸
 Y. Maravin,⁸ I. Narsky,⁸ V. Shelkov,⁸ J. Staeck,⁸ R. Stroynowski,⁸ I. Volobouev,⁸ J. Ye,⁸
 M. Artuso,⁹ A. Efimov,⁹ M. Goldberg,⁹ D. He,⁹ S. Kopp,⁹ G. C. Moneti,⁹ R. Mountain,⁹
 S. Schuh,⁹ T. Skwarnicki,⁹ S. Stone,⁹ G. Viehhauser,⁹ X. Xing,⁹ J. Bartelt,¹⁰ S. E. Csorna,¹⁰
 V. Jain,^{10,§} K. W. McLean,¹⁰ S. Marka,¹⁰ R. Godang,¹¹ K. Kinoshita,¹¹ I. C. Lai,¹¹
 P. Pomianowski,¹¹ S. Schrenk,¹¹ G. Bonvicini,¹² D. Cinabro,¹² R. Greene,¹² L. P. Perera,¹²
 G. J. Zhou,¹² B. Barish,¹³ M. Chadha,¹³ S. Chan,¹³ G. Eigen,¹³ J. S. Miller,¹³
 C. O'Grady,¹³ M. Schmidtler,¹³ J. Urheim,¹³ A. J. Weinstein,¹³ F. Würthwein,¹³
 D. W. Bliss,¹⁴ G. Masek,¹⁴ H. P. Paar,¹⁴ S. Prell,¹⁴ V. Sharma,¹⁴ D. M. Asner,¹⁵
 J. Gronberg,¹⁵ T. S. Hill,¹⁵ D. J. Lange,¹⁵ S. Menary,¹⁵ R. J. Morrison,¹⁵ H. N. Nelson,¹⁵
 T. K. Nelson,¹⁵ C. Qiao,¹⁵ J. D. Richman,¹⁵ D. Roberts,¹⁵ A. Ryd,¹⁵ M. S. Witherell,¹⁵
 R. Balest,¹⁶ B. H. Behrens,¹⁶ W. T. Ford,¹⁶ H. Park,¹⁶ J. Roy,¹⁶ J. G. Smith,¹⁶
 J. P. Alexander,¹⁷ C. Bebek,¹⁷ B. E. Berger,¹⁷ K. Berkelman,¹⁷ K. Bloom,¹⁷ D. G. Cassel,¹⁷
 H. A. Cho,¹⁷ D. S. Crowcroft,¹⁷ M. Dickson,¹⁷ P. S. Drell,¹⁷ K. M. Ecklund,¹⁷ R. Ehrlich,¹⁷
 A. D. Foland,¹⁷ P. Gaidarev,¹⁷ R. S. Galik,¹⁷ B. Gittelman,¹⁷ S. W. Gray,¹⁷ D. L. Hartill,¹⁷
 B. K. Heltsley,¹⁷ P. I. Hopman,¹⁷ J. Kandaswamy,¹⁷ P. C. Kim,¹⁷ D. L. Kreinick,¹⁷
 T. Lee,¹⁷ Y. Liu,¹⁷ G. S. Ludwig,¹⁷ N. B. Mistry,¹⁷ C. R. Ng,¹⁷ E. Nordberg,¹⁷ M. Ogg,^{17,**}
 J. R. Patterson,¹⁷ D. Peterson,¹⁷ D. Riley,¹⁷ A. Soffer,¹⁷ B. Valant-Spaight,¹⁷ C. Ward,¹⁷
 M. Athanas,¹⁸ P. Avery,¹⁸ C. D. Jones,¹⁸ M. Lohner,¹⁸ C. Prescott,¹⁸ J. Yelton,¹⁸
 J. Zheng,¹⁸ G. Brandenburg,¹⁹ R. A. Briere,¹⁹ A. Ershov,¹⁹ Y. S. Gao,¹⁹ D. Y.-J. Kim,¹⁹
 R. Wilson,¹⁹ H. Yamamoto,¹⁹ T. E. Browder,²⁰ F. Li,²⁰ Y. Li,²⁰ J. L. Rodriguez,²⁰
 T. Bergfeld,²¹ B. I. Eisenstein,²¹ J. Ernst,²¹ G. E. Gladding,²¹ G. D. Gollin,²¹ R. M. Hans,²¹
 E. Johnson,²¹ I. Karliner,²¹ M. A. Marsh,²¹ M. Palmer,²¹ M. Selen,²¹ J. J. Thaler,²¹
 K. W. Edwards,²² A. Bellerive,²³ R. Janicek,²³ D. B. MacFarlane,²³ P. M. Patel,²³
 A. J. Sadoff,²⁴ R. Ammar,²⁵ P. Baringer,²⁵ A. Bean,²⁵ D. Besson,²⁵ D. Coppage,²⁵
 C. Darling,²⁵ R. Davis,²⁵ N. Hancock,²⁵ S. Kotov,²⁵ I. Kravchenko,²⁵ and N. Kwak²⁵

*Permanent address: Lawrence Livermore National Laboratory, Livermore,

†Permanent address: BINP, RU-630090 Novosibirsk, Russia.

‡Permanent address: Yonsei University, Seoul 120-749, Korea.

§Permanent address: Brookhaven National Laboratory, Upton, NY 11973.

**Permanent address: University of Texas, Austin TX 78712

¹University of Minnesota, Minneapolis, Minnesota 55455
²State University of New York at Albany, Albany, New York 12222
 ³Ohio State University, Columbus, Ohio 43210
 ⁴University of Oklahoma, Norman, Oklahoma 73019
 ⁵Purdue University, West Lafayette, Indiana 47907
 ⁶University of Rochester, Rochester, New York 14627
⁷Stanford Linear Accelerator Center, Stanford University, Stanford, California 94309
 ⁸Southern Methodist University, Dallas, Texas 75275
 ⁹Syracuse University, Syracuse, New York 13244
 ¹⁰Vanderbilt University, Nashville, Tennessee 37235
¹¹Virginia Polytechnic Institute and State University, Blacksburg, Virginia 24061
 ¹²Wayne State University, Detroit, Michigan 48202
 ¹³California Institute of Technology, Pasadena, California 91125
 ¹⁴University of California, San Diego, La Jolla, California 92093
 ¹⁵University of California, Santa Barbara, California 93106
 ¹⁶University of Colorado, Boulder, Colorado 80309-0390
 ¹⁷Cornell University, Ithaca, New York 14853
 ¹⁸University of Florida, Gainesville, Florida 32611
 ¹⁹Harvard University, Cambridge, Massachusetts 02138
 ²⁰University of Hawaii at Manoa, Honolulu, Hawaii 96822
 ²¹University of Illinois, Champaign-Urbana, Illinois 61801
 ²²Carleton University, Ottawa, Ontario, Canada K1S 5B6
 and the Institute of Particle Physics, Canada
 ²³McGill University, Montréal, Québec, Canada H3A 2T8
 and the Institute of Particle Physics, Canada
 ²⁴Ithaca College, Ithaca, New York 14850
 ²⁵University of Kansas, Lawrence, Kansas 66045

The decay of the τ lepton provides a test of the standard model prediction of the hadronic weak current. The decay $\tau^- \rightarrow 2\pi^-\pi^+3\pi^0\nu_\tau$ [1] is related to $\tau^- \rightarrow 3\pi^-2\pi^+\pi^0\nu_\tau$ and $\tau^- \rightarrow \pi^-5\pi^0\nu_\tau$ by isospin symmetry and to the cross section for $e^+e^- \rightarrow 6\pi$ by the Conserved-Vector-Current (CVC) hypothesis. The decay can therefore be used to test the isospin and CVC predictions. However, these predictions are for the $I = 1$ component of the hadronic weak vector current so any $I = 0$ contribution to the e^+e^- cross-section or any axial-vector contribution to the τ decay through an η intermediate state must be removed before the comparison. The isospin symmetry also relates the relative branching fractions among the four possible isospin states [2], 510 ($4\pi\rho$), 330 (3ρ), 411 ($3\pi\omega$), and 321 ($\pi\rho\omega$), which we denote according to the lowest mass states. The search for possible η and ω substructure will therefore be of particular interest. Any substructure will also be powerful in suppressing hadronic background in the measurement of the ν_τ mass using the six-pion decay. Recently, the ALEPH collaboration [3] reported substantial branching fractions for the decays $\tau^- \rightarrow 2\pi^-\pi^+n\pi^0\nu_\tau (n \geq 3)$ and $2\pi^-\pi^+3\pi^0\nu_\tau$ of $(1.1 \pm 0.4 \pm 0.5) \times 10^{-3}$ and $(2.0 \pm 0.6 \pm 0.6) \times 10^{-3}$, respectively. In this Letter, we present a new result for the branching fraction of $\tau^- \rightarrow 2\pi^-\pi^+3\pi^0\nu_\tau$ and the first observation of $\tau^- \rightarrow \pi^-2\pi^0\omega\nu_\tau$. We assume that all three charged particles in the decay are pions.

The data used in this analysis have been collected from e^+e^- collisions at a center-of-mass energy (\sqrt{s}) of 10.6 GeV with the CLEO II detector at the Cornell Electron Storage Ring (CESR). The total integrated luminosity of the data sample is 4.68 fb^{-1} , corresponding to the production of $4.27 \times 10^6 \tau^+\tau^-$ events. The CLEO II detector has been described in detail elsewhere [4].

We select events with four charged tracks and zero net charge. The distance of closest approach of each track to the interaction point must be within 0.5 cm transverse to the beam and 5 cm along the beam direction. The momentum of each track must be greater than $0.02E_{beam}$ ($E_{beam} = \sqrt{s}/2$) and the polar angle of each track must satisfy $|\cos\theta| < 0.90$, where θ is the polar angle with respect to the beam.

A photon candidate is defined as a crystal cluster with a minimum energy of 40 MeV in the barrel region ($|\cos\theta| < 0.80$) or 150 MeV in the endcap region ($0.80 < |\cos\theta| < 0.95$). The cluster must be isolated by at least 30 cm from the projection of any charged track on the surface of the calorimeter unless its energy is greater than 250 MeV. In addition, the cluster must have a lateral profile of energy deposition consistent with that expected for a photon. A subclass of “high-quality” photons is defined to further discriminate against fake photons; these photons must have a minimum energy of 150 MeV and pass the isolation requirement unless their energy exceeds 250 MeV. All “high-quality” photons must be included in the π^0 reconstruction. The π^0 candidates are selected based on a requirement on $S_{\gamma\gamma} = (m_{\gamma\gamma} - m_{\pi^0})/\sigma_{\gamma\gamma}$, where $\sigma_{\gamma\gamma}$ is the mass resolution calculated from the energy and angular resolution of each photon. We require all π^0 candidates to have $-3.5 < S_{\gamma\gamma} < 2.5$ and be in the barrel; endcap photons are used primarily to veto background events.

Each event is divided into two hemispheres using the plane perpendicular to the thrust axis [5], calculated using both charged tracks and photons. There must be one charged track in one hemisphere recoiling against three charged tracks in the other (1 vs. 3 topology). In the 1-prong hemisphere, the total invariant mass of charged tracks and photons must satisfy $M_1 < 1.0 \text{ GeV}/c^2$. We allow up to two high-quality photons in this hemisphere; for the case of multiple photons, there must be at least one π^0 candidate. For the 3-prong hemisphere, the

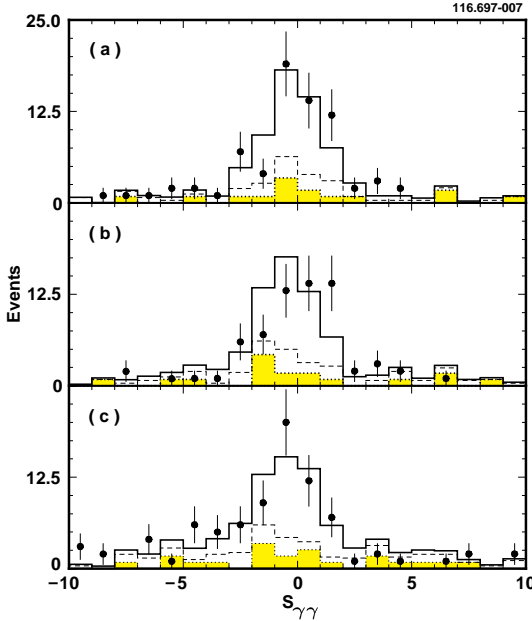


FIG. 1. The $S_{\gamma\gamma}$ distribution for the (a) highest, (b) intermediate, and (c) lowest energy π^0 (see text). The solid histogram is the sum of the signal Monte Carlo and background (dashed), which includes the τ migration and hadronic (shaded) background.

total invariant mass of charged tracks and photons must satisfy $M_3 < M_\tau = 1.777 \text{ GeV}/c^2$ [6]. The magnitude of the total momentum of the particles in the τ rest frame, P^* , must be less than $0.2 \text{ GeV}/c$. In calculating P^* , we ignore initial state radiation and assume that the τ direction is the same as the total momentum vector of the charged tracks and photons in the 3-prong hemisphere. This requirement selects events with tau-like kinematics, suppressing hadronic background and τ migration background for which the momentum vector is not a good approximation of the τ direction. The migration background due to photon conversion is further reduced by a cut on the mass of oppositely charged track pairs (M_{ee}), calculated assuming the electron mass. In the mass calculation, one of the charged particles must be identified as an electron, a particle with a shower energy to momentum ratio in the range, $0.85 < E/P < 1.10$, and, if available, a measured specific ionization loss that is consistent with that expected for an electron. Any event with $M_{ee} < 120 \text{ MeV}/c^2$ is rejected.

There must be at least six photons in the 3-prong hemisphere, forming three exclusive π^0 candidates. If there is more than one combination that satisfies the requirement, the one with lowest total $\chi^2 = \sum_{i=1}^3 [S_{\gamma\gamma}^2]_i$ is selected. The $S_{\gamma\gamma}$ distributions of the three π^0 candidates, classified according to the π^0 energy, are shown in Fig. 1. For each distribution, the $S_{\gamma\gamma}$ of the other two photon pairs must be in their respective signal regions. An enhancement at zero is evident in all three distributions, corresponding to the observation of the decay $\tau^- \rightarrow 2\pi^-\pi^+3\pi^0\nu_\tau$.

The detection efficiency and background from τ migration [7] and hadronic events are calculated with a Monte Carlo (MC) technique. We use the KORALB/TAUOLA program [8] for the τ event simulation and the Lund program [9] for hadronic events. The signal decay is modeled using a mixture of $\tau^- \rightarrow 2\pi^-\pi^+\eta\nu_\tau \rightarrow 2\pi^-\pi^+3\pi^0\nu_\tau$ (39%), $\tau^- \rightarrow \pi^-\pi^+2\pi^0\nu_\tau \rightarrow 2\pi^-\pi^+3\pi^0\nu_\tau$ (11%), and $\tau^- \rightarrow \pi^-\pi^+2\pi^0\omega\nu_\tau \rightarrow 2\pi^-\pi^+3\pi^0\nu_\tau$ (50%). The relative mixtures are

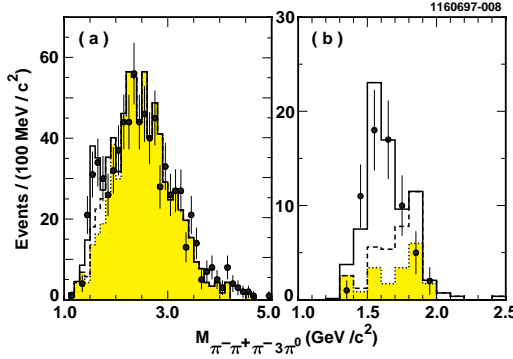


FIG. 2. The invariant mass spectrum of the 3-prong hemisphere (a) before and (b) after the P^* cut is imposed. The solid histogram is the sum of the signal Monte Carlo and background (dashed), which includes the τ migration and hadronic (shaded) background.

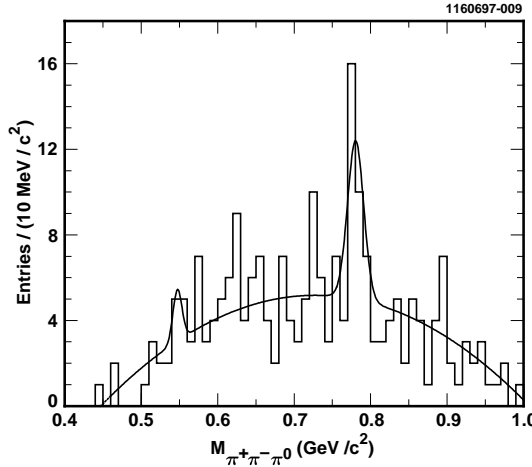


FIG. 3. $\pi^+\pi^-\pi^0$ invariant mass spectrum (6 entries/event). The curve shows a fit to the data.

determined from the measured branching fractions for the first two decays [10]. We assume that the $3\pi\eta$ decays proceed through πf_1 with a spectral function dominated by the form factor of the $a_1(1260)$ resonance [11]. The $3\pi\omega$ system is modeled using phase space. The detector response is simulated using the GEANT program [12]. Since the absolute prediction for low-multiplicity hadronic events may be unreliable, the Lund Monte Carlo is used only to predict the shape of the 3-prong mass spectrum. The hadronic background is calculated by normalizing to the number of data events in the 3-prong hemisphere with $M_3 > 2.0$ GeV before the P^* cut is imposed. The simulation reproduces the $2\pi^-\pi^+3\pi^0$ invariant mass spectrum quite well as shown in Fig. 2. An enhancement of events below M_τ is evident. The signal, background, and detection efficiency are summarized in Table I. Also listed is the branching fraction extracted after correcting for the branching fraction of the 1-prong tag of $(73.0 \pm 0.3)\%$ [6].

The decay $\tau^- \rightarrow 2\pi^-\pi^+3\pi^0\nu_\tau$ can proceed through different intermediate resonances. We have recently observed the decays $\tau^- \rightarrow 2\pi^-\pi^+\eta\nu_\tau$ via $\eta \rightarrow \gamma\gamma$ and $3\pi^0$ and $\tau^- \rightarrow \pi^-\pi^0\eta\nu_\tau$ via $\eta \rightarrow \gamma\gamma$ [10]. For the latter decay, we also expect an η signal in the $\pi^+\pi^-\pi^0$ mass spectrum. Figure 3 shows the $\pi^+\pi^-\pi^0$ mass spectrum (6 entries/event), for which the π^0

TABLE I. Summary of signal, background, detection efficiency, and branching fraction.

Decay Mode	$2\pi^-\pi^+3\pi^0$	$\pi^-\pi^0\omega$
Data	57	$19.4^{+6.8}_{-6.1}$
τ migration	10.2 ± 2.0	2.3 ± 0.2
$q\bar{q}$ background	8.6 ± 2.7	$0.0^{+1.5}_{-0.0}$
Eff (%)	2.16 ± 0.07	1.65 ± 0.09
$B(\times 10^{-4})$	2.85 ± 0.56	$1.89^{+0.74}_{-0.67}$

candidates have been kinematically constrained to the nominal π^0 mass. To reduce the combinatoric background, we exclude events with a $3\pi^0$ mass consistent with that of the η meson. There is an enhancement in the ω mass region corresponding to the first observation of the decay $\tau^- \rightarrow \pi^-2\pi^0\omega\nu_\tau$. There is also an indication of a signal for $\eta \rightarrow \pi^+\pi^-\pi^0$, although not statistically significant. To extract the branching fractions, the spectrum is fitted using a binned maximum likelihood technique with Gaussians for the ω and η signals and a second-order polynomial background. The ω and η masses and widths have been constrained to the Monte Carlo expectations. The result for $\tau^- \rightarrow \pi^-2\pi^0\omega\nu_\tau$ is summarized in Table I. If we interpret the small η excess as signal, the branching fraction extracted for $\tau^- \rightarrow \pi^-2\pi^0\eta\nu_\tau$ is consistent with the expectation [10].

There are several sources of systematic errors as summarized in Table II. The uncertainty in the photon detection efficiency is estimated by varying the photon selection criteria. The systematic error in the decay modeling includes the uncertainties in the branching fractions of $\tau^- \rightarrow 2\pi^-\pi^+\eta\nu_\tau$ and $\pi^-2\pi^0\eta\nu_\tau$ [10] and the modeling of the πf_1 and $3\pi\omega$ systems. The latter uncertainty is estimated from the difference in the detection efficiency between the default models and the models based on a πf_1 phase space and a $\pi\rho\omega$ resonance with mass of 1600 MeV/c² and width of 235 MeV/c². The uncertainty in the background shape in the $\pi^+\pi^-\pi^0$ mass spectrum is estimated by using different orders of polynomial. As a check of the hadronic background estimate, the branching fraction for the decay $\tau^- \rightarrow 2\pi^-\pi^+3\pi^0\nu_\tau$ has been measured using a lepton tag and the result is consistent with that for the non-lepton tag. Including the systematic errors in quadrature, the final results are:

$$\begin{aligned}
 B(\tau^- \rightarrow 2\pi^-\pi^+3\pi^0\nu_\tau) &= (2.85 \pm 0.56 \pm 0.51) \times 10^{-4} \\
 B(\tau^- \rightarrow \pi^-2\pi^0\omega\nu_\tau) &= (1.89^{+0.74}_{-0.67} \pm 0.40) \times 10^{-4},
 \end{aligned}$$

where the first error is statistical and the second is systematic.

We can test isospin symmetry [2] by comparing the fractions of the $I = 1$ component of the six-pion decay into $2\pi^-\pi^+3\pi^0$ and $3\pi^-2\pi^+\pi^0$ states,

$$f_{2\pi^-\pi^+3\pi^0} = \frac{B(\tau^- \rightarrow 2\pi^-\pi^+3\pi^0\nu_\tau)}{B(\tau^- \rightarrow (6\pi)^-\nu_\tau)}$$

and similarly for $f_{3\pi^-2\pi^+\pi^0}$, where $B(\tau^- \rightarrow (6\pi)^-\nu_\tau)$ is the sum of the three branching fractions, $B(\tau^- \rightarrow 2\pi^-\pi^+3\pi^0\nu_\tau)$, $B(\tau^- \rightarrow 3\pi^-2\pi^+\pi^0\nu_\tau)$, and $B(\tau^- \rightarrow \pi^-5\pi^0\nu_\tau)$. The latter branching fraction has not yet been measured. However, we expect the branching fraction

TABLE II. Summary of systematic errors (%).

Mode	$2\pi^-\pi^+3\pi^0$	$\pi^-2\pi^0\omega$
Luminosity	1	1
Cross-section	1	1
τ migration	5	4
$q\bar{q}$ background	5	9
Tracking	4	4
Photon eff.	15	15
Decay model	4	8
Fitting	-	5
Eff (MC stat.)	3	6
Total	18	21

to be small from CVC using the measured cross section of $e^+e^- \rightarrow 3\pi^+3\pi^-$. Sobie [13] and Rouge [14] have performed an isospin analysis of these decays and concluded that there is a discrepancy between the measured decay branching fractions and the isospin expectation. However, the authors did not correct for the axial-vector contributions from the decays $\tau^- \rightarrow 2\pi^-\pi^+\eta\nu_\tau$ and $\pi^-2\pi^0\eta\nu_\tau$. We correct for these contributions using our recent measurements of the branching fractions, $(3.5^{+0.7}_{-0.6} \pm 0.7) \times 10^{-4}$ and $(1.4 \pm 0.6 \pm 0.3) \times 10^{-4}$ [10]. Figure 4 shows $f_{2\pi^-\pi^+3\pi^0}$ vs. $f_{3\pi^-2\pi^+\pi^0}$ with our new measurement of $B_V(\tau^- \rightarrow 2\pi^-\pi^+3\pi^0\nu_\tau) = (1.41 \pm 0.76) \times 10^{-4}$ and the world average measurement [6] of $B_V(\tau^- \rightarrow 3\pi^-2\pi^+\pi^0\nu_\tau) = (1.39 \pm 0.55) \times 10^{-4}$, where the subscript indicates that this is the vector component of the branching fraction. The measurement is in good agreement with the isospin expectation. Because the η and ω intermediate states saturate the decay $\tau^- \rightarrow 2\pi^-\pi^+3\pi^0\nu_\tau$, we can also test the isospin prediction using our measurement of $B(\tau^- \rightarrow 2\pi^-\pi^+3\pi^0\nu_\tau)$ from the decay $\tau^- \rightarrow \pi^-2\pi^0\omega\nu_\tau$. With the assumption that $B(\tau^- \rightarrow \pi^-5\pi^0\nu_\tau)$ is negligible, our measurement of $B_\omega(\tau^- \rightarrow 2\pi^-\pi^+3\pi^0\nu_\tau) = (1.68 \pm 0.72) \times 10^{-4}$ is consistent with the isospin expectation as shown in Fig. 4. The result prefers the dominance of the [321] ($\pi\rho\omega$) isospin state over the [411] ($3\pi\omega$) state; we are not able to distinguish the two states from the $\pi\pi^0$ mass spectrum. Our measurement of $B(\tau^- \rightarrow 2\pi^-\pi^+3\pi^0\nu_\tau)$ can also be compared with the CVC predictions by Sobie [13] and Eidelman [15], $B(\tau^- \rightarrow 2\pi^-\pi^+3\pi^0\nu_\tau) = (1.9 - 7.3) \times 10^{-4}$ and $(2.5 \pm 0.4) \times 10^{-4}$, respectively. Our result is somewhat below the predictions, indicating that there could be a substantial $I = 0$ contribution from $e^+e^- \rightarrow \eta\pi^+\pi^-\pi^0$ to $e^+e^- \rightarrow 2\pi^+2\pi^-2\pi^0$ that must be removed before calculating the CVC predictions.

In conclusion, the decay $\tau^- \rightarrow 2\pi^-\pi^+3\pi^0\nu_\tau$ has been observed. The branching fraction is in a good agreement with the isospin expectation [13,14], but smaller than the ALEPH measurement [3]. We have also observed an ω signal in the six-pion system, corresponding to the decay $\tau^- \rightarrow \pi^-2\pi^0\omega\nu_\tau$. Within the statistical precision, the contribution from this decay together with those [10] from $\tau^- \rightarrow 2\pi^-\pi^+\eta\nu_\tau$ and $\pi^-2\pi^0\eta\nu_\tau$ saturate the decay $\tau^- \rightarrow 2\pi^-\pi^+3\pi^0\nu_\tau$.

We gratefully acknowledge the effort of the CESR staff in providing us with excellent luminosity and running conditions. This work was supported by the National Science Foun-

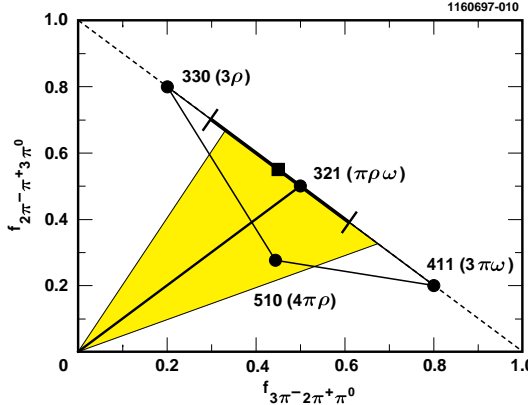


FIG. 4. $f_{2\pi^-\pi^+3\pi^0}$ vs. $f_{3\pi^-2\pi^+\pi^0}$. The solid line from the origin uses the CLEO II result on $B_V(\tau^- \rightarrow 2\pi^-\pi^+3\pi^0\nu_\tau)$ and the world average measurement of $B_V(\tau^- \rightarrow 3\pi^-2\pi^+\pi^0\nu_\tau)$ (see text). The shaded area indicates the one standard deviation region. The square with diagonal error bar uses the CLEO II measurement of $B(\tau^- \rightarrow 2\pi^-\pi^+3\pi^0\nu_\tau)$ from the decay $\tau^- \rightarrow \pi^-2\pi^0\omega\nu_\tau$. The triangular region indicates the isospin expectation. Unitarity requires the fractions to be below the dashed line.

dation, the U.S. Department of Energy, the Heisenberg Foundation, the Alexander von Humboldt Stiftung, Research Corporation, the Natural Sciences and Engineering Research Council of Canada, and the A.P. Sloan Foundation.

REFERENCES

- [1] In this paper charge conjugate states are implied.
- [2] A. Pais, Ann. Phys. **9**, 548 (1960). For an isospin state $[n_1, n_2, n_3]$, n_3 is the number of subsystems of three pions with $I = 0$, $n_2 - n_3$ is the number of subsystems of two pions with $I = 1$, and $n_1 - n_2$ is the number of remaining single pions.
- [3] D. Buskulic *et al.*, Z. Phys. C **70**, 579 (1996).
- [4] Y. Kubota *et al.*, Nucl. Instrum. Methods A **320**, 66 (1992).
- [5] E. Farhi, Phys. Rev. Lett. **39**, 1587 (1977).
- [6] R. Barnett *et al.*, Review of Particle Properties, Phys. Rev. D **54**, 1 (1996).
- [7] The dominant migration background in the decay $\tau^- \rightarrow 2\pi^-\pi^+3\pi^0\nu_\tau$ ($\pi^-\pi^0\omega\nu_\tau$) is from $\tau^- \rightarrow 2\pi^-\pi^+2\pi^0\nu_\tau$ ($\pi^-\pi^0\omega\nu_\tau$).
- [8] S. Jadach and Z. Was, Comp. Phys. Comm. **36**, 191 (1985); *ibid.* **64**, 267 (1991); S. Jadach, J. H. Kuhn, and Z. Was, *ibid.* **64**, 275 (1991).
- [9] T. Sjöstrand and M. Bengtsson, Comp. Phys. Comm. **43**, 367 (1987).
- [10] T. Bergfeld *et al.*, CLNS 97/1489 (submitted to Phys. Rev. Lett.).
- [11] B.A. Li, Phys. Rev. D **55**, 1436 (1997).
- [12] R. Brun *et al.*, CERN Report No. CERN-DD/EE/84-1, 1987 (unpublished).
- [13] R.J. Sobie, Z. Phys. C **69**, 99 (1995).
- [14] A. Rouge, Z. Phys. C **70**, 65 (1996).
- [15] S.I. Eidelman and V.N. Ivanchenko, Nucl. Phys. B (Proc. Suppl.) **55C**, 181 (1997). (Proceedings of the Fourth International Workshop on Tau Lepton Physics, Estes Park, Colorado, 1996, edited by J.G. Smith and W. Toki.)